OTC 25210-MS

Investigating Modern Ultra Deepwater Sedimentary Processes in the Central Gulf of Mexico Using High Resolution Geophysical Data

Maria I. Prieto, The University of Texas at Austin, Dr. Lorena Moscardelli, Statoil RDI, and Dr. Lesli Wood, Bureau of Economic Geology

Abstract

A detailed geomorphologic and shallow stratigraphic interpretation was performed in three different geomorphological domains of the ultra-deepwater region of the central Gulf of Mexico (GOM) using a set of high resolution bathymetry and subbottom profiles that were acquired at four major oil fields in the Green Canyon and Mississippi Canyon protraction areas. The seafloor expression of the study areas allowed defining three different geomorphological provinces: Minibasin, Sigsbee Escarpment and Disconnected Canopy Province. The geomorphological expression of these provinces is primarily the result of the dynamic behavior of the underlying salt, in which these regions experienced different degrees and types of substrate deformation. Structural deformation affecting these areas has been very dynamic through time enhancing the occurrence of both regional and localized gravity-induced deposits. Regions of high relief along diapiric slopes (e.g.: Sigsbee Escarpment) are affected by headwall failures and the near seafloor stratigraphy reveals the complex dynamic of eroded and re-deposited sediments that have been affected by both gravity- and current-driven processes. This study seeks to improve our understanding of how local bathymetric variabilities (linked to underlying structural controls) interact with gravity-driven and current-controlled processes in the ultra-deepwater region of the GOM to generate the near seafloor stratigraphic record that is observable in our study areas.

Introduction

Understanding of sedimentary processes affecting ultra-deepwater environments is particularly challenging since existing data sets (well and seismic data) cover limited areas and are usually difficult to access due to their proprietary nature. Gravity-driven and current-controlled processes and associated deposits are known to occur as part of abyssal strata of ancient oceans; however, few modern analogs exist to explain how these processes and deposits form. In 2011 a set of high resolution geophysical data, including multibeam bathymetry, side-scan sonar images and chirp subbottom profiles, were donated by BP America to a number of universities. The surveys were acquired in the central Gulf of Mexico (GOM) during 2001 for geohazards evaluation purposes at water depths of 3700-7100 ft, and cover four major fields: Atlantis, Mad Dog and Holstein in the Green Canyon protraction area, and Thunder Horse in the Mississippi Canyon protraction area (Fig. 1).

In this work, preliminary analysis of these data is performed to provide with a brief description of the main structural and stratigraphic elements that are present in these regions. Near seafloor stratigraphic units in the study areas are characterized based on their seafloor geomorphological expression and acoustic response. The high vertical and horizontal resolution associated with the data enabled us to map in detail stratal relationships, as well as to provide with a detailed view of the main structural and geomorphological elements that are present in the shallow subsurface.

Three submarine deepwater geomorphological provinces were defined based on the character of the underlying structures (salt tectonics) and the four study areas were grouped into one of these subcategories: 1) Minibasin Province (Holstein), 2) Sigsbee Escarpment (Mad Dog and Atlantis) and 3) Disconnected Canopy Province (Thunder Horse). Each geomorphological province has morphological characteristics that influenced the way in which currents and gravity-induced processes interact with the existing bathymetry.

Data and Methods

A four-survey dataset of ultra-high resolution geophysical data were collected for BP America in 2001 for geohazards evaluation purposes. The data was acquired using an Autonomous Underwater Vehicle (AUV) along grids of 500m and 200m line

spacing within the survey areas, keeping a constant distance of ~130-160 ft above the seafloor [1]. The data collected include three types of surveys: multibeam bathymetry, side-scan sonar data and subbottom profiles. The multibeam bathymetry was gridded at a 5m horizontal resolution using Z-map© software. Side-scan sonar data imaged the seafloor by emitting fan-shaped pulses and recording the intensity of the reflection. A composite digital sonar mosaic was generated using CARIS Hips and Sips© software. The subbottom profiles provide high-resolution images of the subsea floor strata down to ~225 m (738 ft) deep. The high frequency content of the chirp subbottom profiles (2-8 kHz) enables high vertical resolution (~3 ft) of stratal relationships [1]. The profiles were loaded into Openworks© and interpreted using DecisionSpace© software. Together, these three types of data provide a detailed view of the structural, stratigraphic and geomorphological elements that are present in the shallow subsurface of the four study areas. Table 1 indicates the total area covered by each of the surveys and the total length of the acquired lines within individual grids.

Table 1 – Area coverage of ultra-high resolution geophysical data

Survey	Geomorphological Province	Area (km^2)	*Line Length (km)
Holstein	Minibasin	67	1310
Mad Dog	Sigsbee Escarpment	133	2823
Atlantis	Sigsbee Escarpment	185	4000
Thunder Horse	Disconnected Canopy Province	266	5450

* Addition length of all lines within each survey/grid

Multibeam bathymetric maps were generated to identify geomorphological features (e.g.: slumps, headscarps, debris flows, fault scarps, furrows, etc.) that were later placed into the context of each of the pre-defined geomorphological domains. Observations made on bathymetric maps were integrated with side-scan sonar mosaic interpretation, allowing us to identify and increase the level of geomorphological detail in some areas. The interpretation of subbottom profiles was based on the difference of the acoustic response (high vs low amplitude reflections as well as internal seismic character), and the observed variability was linked to the occurrence of different depositional units. The overall stratigraphic framework was tighten to previous work performed within the Mad Dog and Atlantis surveys [2]–[5]. Three sedimentary sequences that were previously identified by Taylor (2001) were also recognized using the data in the Disconnected Canopy Province in the Mississippi Canyon area. The generation of time structural maps and isochron maps of sedimentary units enabled us to document the vertical and lateral evolution of the main stratigraphic units, as well as to pinpoint the relative timing of key events.

Regional Setting

The present topography and seafloor morphology of the slope region in the central GOM area is the result of the interplay between shelf-edge progradation, shale and salt diapirism, sediment loading, dynamic topography of salt, subsalt deformation and slope instability induced mass movements [6], [7]. The Sigsbee Escarpment, a ~2300 ft relief bathymetric feature, represents the boundary between the base of the continental slope and the upper continental rise; this boundary also defines the downslope limit of the shallow allochtonous salt in the GOM [8], [9]. Towards the abyssal regions the relief is mainly smooth, however at the base of the escarpment, big sedimentary furrows that run parallel to the strike direction have been previously mapped [3], [10], [11]. These furrows run for several kilometers, and in the Mad Dog and Atlantis areas they are 20 to 30 m wide and 3 to 8 m deep. Strong bottom currents that flow parallel to these furrows have been measured in the abyssal portion of the Sigsbee Escarpment [3]. Recent measurements indicate that deepwater bottom currents in this region can reach more than 100 cm/s [3], [10], [12], [13]. To the northeast, a prominent U-shaped erosional feature cutting through the shelf break represents the Mississippi Canyon (Fig.1). The canyon is 30 km wide and it was the major sedimentary pathway that linked the continental shelf to the Mississippi Fan. East from the canyon, the seafloor morphology is influenced by underlying "pancake-shaped" (5-15 km wide) salt domes that become more scattered and smaller in size in a basinward direction (Fig.1) [6].

Deepwater currents in the Gulf of Mexico. The Loop Current is a warm-water surface current that originates in the Caribbean Sea and enters the GOM through the Yucatan Strait (National Oceanic and Atmospheric Administration). Upon entering the gulf, the Loop Current flows in a clockwise direction, until it exits the gulf through the Florida Strait. Within the gulf, eddies are detached from the Loop Current and disperse into the western GOM [14], [National Oceanic and Atmospheric Administration]. Together, the Loop Current and associated eddies dominate the upper (surface to depths of 500 to 1000m) circulation within the gulf [15], [16]. Studies that have attempted to understand the dynamics of bottom circulation within the gulf at depths greater than 1000m, suggest that the Loop Current and associated eddies influence the hydrodynamics of the deepest portions of the water column within the GOM [12], [13], [15]–[17]. In addition, the hydrodynamic behavior of deepwater currents in the GOM is also dominated by topographic Rossby waves that run along the slope and that are highly influenced by bathymetric barriers such as the Sigsbee Escarpment [12], [13]. Rossby waves can reach velocities >90cm/s at

water depths of 2000m and are believed responsible for a variety of erosional and depositional features that are associated with the Sigsbee Escarpment.

Description of geomorphological provinces

The study areas are located within three geomorphological domains in the GOM: Minibasin, Sigsbee Escarpment and Disconnected Canopy Province. These three provinces experienced different degrees of substrate deformation linked to specific underlying structural controls. Bottom- current activity also affected these areas differently and multiple sedimentary pathways have also been present through geologic time. In terms of structural controls, it is the underlying salt that plays the largest role in deforming and destabilizing the seafloor. This effect is felt most dramatically in the Sigsbee Escarpment, where salt is actively advancing southward [8], [9]. This generates stresses at the seafloor, creating fault systems that are oriented both parallel and perpendicular to the slope and that have clear sea floor expression as shown in the high resolution bathymetry data (Fig. 2). Deformation also favors the initiation of sediment mass failures that are triggered by steepness of the slope. Bottom-currents seem to preferentially run parallel to the Sigsbee Escarpment gouging furrows and remobilizing sediments across this boundary. Within the Minibasin Province, the majority of structural movement seems to be vertical due to inflation of diapirs [7]. The uplift of salt diapirs can completely isolate an area (minibasin), but sediments infill by a combination of suspension, gravity- and current-controlled processes is not uncommon. The following section describes the main geomorphological characteristics that define each of these geomorphological provinces and theirs shallow stratigraphy infill.

Sigsbee Escarpment (southeastern portion of Green Canyon area; Mad Dog and Atlantis surveys). The geomorphological expression of this area is primarily influenced by the dynamic behavior of the allochtonous salt body that causes oversteeping of the Sigsbee Escarpment [1], [9]. The Mad Dog and Atlantis fields are located at water depths ranging from 4100 ft -7100 ft and share many commonalities but also present some differences in terms of geomorphological characteristics (Fig. 2). The spatial changes in the structural framework along the escarpment influence the seafloor processes and deposits in both areas. Above the escarpment, in the landward direction, the geomorphology tends to be subtler; however, a series of underlying normal faults influence the location of sedimentary pathways that are sometimes parallel to the escarpment (e.g.: Mad Dog) and other times perpendicular to the escarpment (e.g.: Atlantis). Steep slope angles and a multitude of slump scars along the depositional profile characterize the escarpment region. Large amphitheater-shaped slumps, as well as smaller slump scars are present both in Mad Dog and Atlantis. Numerous gully incisions are also observed in areas presenting steeper slopes (e.g.: Atlantis). Most of the slumped scars transition downslope into a variety of sediment masses that in some cases allow for recognition of individual blocks (Fig. 3). Seawards of the escarpment front (abyssal plain), debris flows that originate from the slumped region are visible (Fig. 2). Some of these debris flows can be connected upslope to the sedimentary pathways but many others are localized collapsed features derived from the upper part of the slope. Downslope, the presence of big furrowed erosional features, that are oriented parallel to the escarpment, suggests that bottom-currents running parallel to the slope managed to rework some of the mass wasting units into a furrowed topography (Fig. 3 and Fig. 4). The presence of this furrowed texture is evident both in the bathymetry and side scan images, as well as in the subbottom profiles [1], [18], [19].

Sedimentation along the lower continental slope in the vicinity of the Sigsbee Escarpment was described by Slowey et al. (2003) as a thick succession of late Quaternary-aged hemipelagic sediments. Inboard the escarpment, subbottom profiles show continuous parallel reflections that are cut and offset by normal faults but the base of this stratigraphic unit contains mass transport deposits (MTD) both in Mad Dog and Atlantis (Figs. 3 and 5). The MTDs are recognizable in the subbottom profiles by the presence of chaotic semi-transparent seismic facies (Fig. 3). Time structural maps at the top of this unit and the isochron map of this deposit in the Mad Dog area; illustrate the influence that the underlying salt exerts in defining sedimentary pathways (Fig. 5A and Fig. 5C).

The parallel reflections that are on top of this MTD suggest that the deposits are hemipelagic, this interpretation is also supported by core data that was previously acquired in this area [2], [5]. The inboard NE-SW trending graben in the Mad Dog area confined sediments that resulted from slumping within the walls of the structure, as well as sediments that came from upslope sources and that were able to make their way basinward following the path of the structural lows (Fig. 2 and Fig. 3). This sedimentary pathway managed to deliver sediments toward the abyssal plain, even though a portion of the sediments were sequestered within the confines of the structure. To the east, Atlantis shows a slightly different arrangement in which the main sedimentary pathway and associated underlying structure trend perpendicular to the Sigsbee Escarpment. In this case, the sedimentary pathway seems to be delivering sediments directly into the basin as evidenced by the presence of an extensive debris flow field in the abyssal plain that can be directly connected to the distal end of the pathway (Fig. 2B).The western portion of the escarpment in the Atlantis region shows large, amphitheater-shaped headscarps and dendritic morphologies where gully incisions are common. In contrast, the eastern portion of the Atlantis escarpment presents smaller headscarps with reduced run-up distances for the slumped material (Fig. 2B). It is also interesting to notice that the furrowed textures that are observed in the abyssal plain in the Atlantis region are less accentuated than their equivalents in the Mad Dog area. At the same time, small lobate features that seem to be connected to the escarpment region by channelized features are present in the eastern portion of the Atlantis region but these features are completely absent in the Mad Dog area. Young et al. (2003) described in detail the evolution of mass wasting events within the Atlantis and Mad Dog areas. The peak stage

of failures in the Sigsbee Escarpment occurred over the last 25, 000 yrs with a decrease in activity during the last 8,000 yrs. [4]. The variability in the distribution of seismic facies and morphologies in the Atlantis and Mad Dog areas is indicative of a dynamic ultra-deepwater environment in which a multitude of factors influenced the final character of the deposits. Such factors include underlying structural configuration (e.g., orientation of structures), type of sediment supply, type of substratum and current intensity among many others.

Minibasin Geomorphologic Province (Holstein survey). The Holstein field is located in the minibasin's outer-canopy contractional province in the Green Canyon area as defined by Hudec et al. (2009), (Fig. 1). The field lies at water depths ranging from 3648 ft. to 4485 ft. and it is formed by a large, steep, southeasterly dipping, monoclinal structure, where sediments are being deposited in a ponded salt basin [20]. In this region, the bathymetry is smoother than the Sigsbee Escarpment, slope gradients are not as abrupt, and evidence of gravity-induced deposits acting in the seafloor is not that obvious (Fig. 6). There are several normal faults that have seafloor expression and shallow vertical fault displacement ranges from 10 to 100 ft. These faults are arranged in a concentric pattern defining the minibasin's western edge. The available survey in this study only covers the southwestern rim of the Holstein minibasin (Fig. 1).

Seismic subbottom profiles in the Holstein region show intercalations of parallel continuous reflections and chaotic semitransparent units interpreted as MTDs (Fig. 7). These profiles show the presence of at least three MTDs that have been named from oldest to youngest: HOL-MTD_1, HOL-MTD_2 and HOL-MTD_3. In cross sectional view, their thicknesses seem to decrease from oldest to youngest even though HOL-MTD_1 was not completely imaged by the survey. The time structural map of the top surface of HOL-MTD_1 was generated to visualize the extent of this unit within the study area (Fig. 8A). The surface that defines the top of HOL-MTD_1 dips toward the north and seismic subbottom profiles show a prominent MTD occupying the main axis of the minibasin. This unit wedges against the steepest portions of the minibasin toward the west (Fig. 7B). Due to lack of data coverage, it is still unclear if the source material for the MTDs that were imaged by this survey is extrabasinal or intrabasinal in nature (detached versus attached MTD) [21], [22]. However, over-steepening of the flanks of the minibasin due to halokinesis is a prime suspect as a potential triggering mechanism. Isochron maps for HOL-MTD_2 and HOL-MTD_3 were generated and are shown in figures 8B and 8C. The isochron map of HOL-MTD_2 (Fig. 8B) shows that there is a depocenter to the north and what seems to be a narrow sedimentary conduit that extends toward the south. The regional bathymetric map (Fig.1) suggests that the Holstein area contains an open flank toward the south that could have allowed for sediments to spill outside the minibasin. The isochron map of HOL-MTD_3 indicates that this is the thinnest of all three mass wasting units and that its areal extent is constrained to the boundaries of the minibasin. The apparent limited extension of HOL-MTD_3 can be linked to a smaller sediment volume or to an inherited topography that acted as a flow barrier preventing sediments to extend southwards in this part of the basin.

Seismic subbottom profiles also show the presence of undulating features below HOL-MTD_2 (Fig. 9). Based on their morphology, these features are interpreted as sediment waves. These sediment waves are present within the area located in between the two bathymetric highs at the south edge of the minibasin. They have an average wavelength (defined as the distance between two consecutive crests) of 200m and a wave height (length representing the height of the wave crest) of about 10m. The profile showing sediment waves at Holstein has an N-S orientation, meaning that the crests are aligned in an E-W orientation. This suggests that the direction of flow generating sediment waves was from north to south. Sediment waves at Holstein are asymmetric showing thicker beds in the upslope direction. These thicker wave flanks are indicative of wave upslope migration (upcurrent) in the opposite direction to the dominant flow. The morphology, orientation and scale of these deepwater sediment waves suggest that these features could have been formed by the action of turbidity currents flowing through the minibasin [23]. The narrowing of the southern flank of the Holstein minibasin could have favored the establishment of hydrodynamic conditions in which the velocity of the turbidity currents were significantly enhanced allowing for the formation of these deepwater sediment waves.

Disconnected Canopy Geomorphologic Province (Thunder Horse survey). Thunder Horse is located within the lower continental slope to the east of the Mississippi Canyon in water depths ranging from 5250ft - 6645ft. This area lies in the disconnected salt stock canopy province, where large deeply rooted salt bodies flare outward [24]. A major shallow allochthonous salt feature, called the Thunder Horse diapir lies beneath the study area and has a positive bathymetric expression at the seafloor [25], [26]. The Thunder Horse bathymetric survey clearly shows the presence of two different geomorphologic areas (Fig. 10A). Towards the north, the seafloor is influenced by the underlying salt tower and presents a higher elevation and domal appearance. The southern portion of the study area is 25 ft lower in elevation and presents a slope that dips toward the southeast. The general texture of the seafloor is hummocky; however there is a transitional area that defines the boundary between the domal structure and the lower elevations toward the southeast where the seafloor is smoother. The slope follows a general northwest-southeast trajectory; traction marks and pressure ridges suggest that sediment flow was active in this region in the recent geologic past. The dip magnitude map of the seafloor highlights the presence of debris flows running downslope (Fig. 10B). There are also concentric normal faults near the top of the domal structure some of which seem to be linked to mass failures.

Seismic subbottom profiles in the Thunder Horse region showcase intercalations of acoustically semi-transparent units and high-amplitude parallel continuous reflections (Fig. 11). The chaotic semitransparent units are interpreted as MTDs while the parallel, continuous reflections are linked to a combination of hemipelagic and turbiditic sedimentation. The thickness of

the various stratigraphic units in this region is uneven marked by unconformities defining three main sedimentary sequences [27]. Thicker intervals sometimes occur in the relative lows associated to the hummocky surface (Fig. 11). These changes in thickness, previously interpreted as amorphous lenses of sediment [27], trend parallel to the regional slope.

Conclusions

The three geomorphological provinces within the study area experienced different degrees and types of substrate deformation. Bottom- current activity also affected these areas differently based on their interaction with local bathymetric variabilities. Development of sedimentary pathways was strongly influenced by the character of underlying structural elements since halokinetic deformation has the capacity to shift the location of depocenters and relative structural lows. In terms of mass wasting events, it is the underlying salt that plays the largest role in deforming and destabilizing the seafloor. This effect is felt most dramatically in the Sigsbee Escarpment, where salt is actively advancing southward. Local structural controls generate stresses at the seafloor, creating fault systems that can trend parallel to the slope and that have clear sea floor expression. The associated deformation and uplifting also favors the initiation of mass failures that flow perpendicular to the general slope orientation into the abyssal plain. Bottom-currents seem to preferentially run parallel to the Sigsbee Escarpment gouging furrows and remobilizing sediments across this boundary. It is the local structural configuration in these provinces that allows for current-controlled processes to be active enough in these water depths to be capable of reworking sediments. As it has been previously interpreted, the presence of bathymetric irregularities in the escarpment region can trigger the development of high-velocity, Rossby waves that have the capacity to rework sediments at these water depths. Although it is difficult to unequivocally identify current-controlled deposits (sediments waves can also be formed by enhanced turbidity currents), the presence of erosional features such as furrows near the escarpment front and moats and scours that are often trending parallel to the slope is a strong indicator that current-controlled processes played an important role in the formation of these features.

Acknowledgements

This work is part of the dissertation of Maria I. Prieto under the supervision of Drs. Lorena Moscardelli and Lesli Wood. This research was made possible thanks to the donation of data by BP America and through the generous members of the Quantitative Clastics Laboratory (QCL) consortia and of the University of Texas Institute for Geophysics. The University of Texas at Austin acknowledges support of this research by Landmark Graphics Corporation via the Landmark University Grant Program. Publication authorized by the Director, Bureau of Economic Geology, Jackson School of Geosciences, The University of Texas at Austin.

References

[1] Y.-D. Eddy Lee and R. a. “Tony” George, “High-resolution geological AUV survey results across a portion of the eastern Sigsbee Escarpment,” *Am. Assoc. Pet. Geol. Bull.*, vol. 88, no. 6, pp. 747–764, Jun. 2004.

[2] J. Brand, D. Lanier, M. Angell, and K. Hanson, “Indirect Methods of Dating Seafloor Activity: Geology, Regional Stratigraphic Markers, and Seafloor Current Processes,” *Offshore Technol. Conf.*, 2003.

[3] A. Niedoroda, C. Reed, and L. Hatchett, “Bottom Currents, Deep Sea Furrows, Erosion Rates, and Dating Slope Failure-Induced Debris Flows along the Sigsbee Escarpment in the Deep Gulf of Mexico,” *Offshore Technol. Conf.*, pp. 0–5, 2003.

[4] A. Young, D. Bryant, and D. Slowey, “Age dating of past slope failures of the Sigsbee Escarpment within Atlantis and Mad Dog developments,” *Offshore Technol. Conf.*, no. 2, 2003.

[5] N. Slowey, B. Bryant, D. Bean, A. Young, and S. Gartner, “Sedimentation in the vicinity of the Sigsbee escarpment during the last 25,000 years,” in *Proceedings, Offshore Technology Conference,*, 2003, vol. 15159, pp. 1–15.

[6] J. Y. Liu, W. R. Bryant, S. E. Mahmoud, E. A. Pessagno Jr, and J. P. Bhattacharya, “Sea floor morphology and sediment paths of the northern Gulf of Mexico deepwater,” *Spec. Publ.*, vol. 68, pp. 33–46, 2000.

[7] M. R. Hudec, M. P. a. Jackson, and D. D. Schultz-Ela, “The paradox of minibasin subsidence into salt: Clues to the evolution of crustal basins,” *Geol. Soc. Am. Bull.*, vol. 121, no. 1/2, pp. 201–221, 2009.

[8] A. Niedoroda, C. Reed, and L. Hatchett, “Analysis of past and future debris flows and turbidity currents generated by slope failures along the Sigsbee Escarpment in the deep Gulf of Mexico,” *Offshore Technol. Conf.*, 2003.

[9] D. Orange, M. Angell, and J. Brand, "Geologic and shallow salt tectonic setting of the Mad Dog and Atlantis fields Relationship between salt, faults, and seafloor geomorphology," *Lead. Edge*, vol. 23, pp. 354–365, 2004.

[10] W. Bryant and D. Bean, "Massive bed-forms, mega-furrows, on the continental rise at the base of the Sigsbee Escarpment, northwest Gulf of Mexico," *Gulf Coast Assoc. Geol. Soc. Trans.*, vol. L, p. 2000, 2000.

[11] a. R. Viana, W. Almeida, M. C. V. Nunes, and E. M. Bulhoes, "The economic importance of contourites," *Geol. Soc. London, Spec. Publ.*, vol. 276, no. 1, pp. 1–23, Jan. 2007.

[12] P. Hamilton, "Topographic Rossby waves in the Gulf of Mexico," *Prog. Oceanogr.*, vol. 82, no. 1, pp. 1–31, Jul. 2009.

[13] P. Hamilton, "Deep-Current Variability near the Sigsbee Escarpment in the Gulf of Mexico," *J. Phys. Oceanogr.*, vol. 37, no. 3, pp. 708–726, Mar. 2007.

[14] L.-Y. Oey, T. Ezer, and H. Lee, "Loop Current, rings and related circulation in the Gulf of Mexico: A review of numerical models and future challenges," *Circ. Gulf Mex. Obs. Model. Am. Geophys. Union*, vol. 161, pp. 31–56, 2005.

[15] L.-Y. Oey, "Loop Current and Deep Eddies," *J. Phys. Oceanogr.*, vol. 38, no. 7, pp. 1426–1449, Jul. 2008.

[16] M. Inoue, S. E. Welsh, L. Rouse, and E. Weeks, "Deepwater Currents in the Eastern Gulf of Mexico : Observations at 25 . 5°N and 87°W," *U.S. Dep. Inter. Miner. Manag. Serv. Gulf Mex. OCS Reg.*, 2008.

[17] L.-Y. Oey and P. Hamilton, "Ultra-deep circulation processes in the Gulf of Mexico," 2011.

[18] J. E. Damuth and D. E. Hayes, "Echo character of the east Brazilian continental margin and its relationship to sedimentary processes," *Mar. Geol.*, vol. 24, no. 2, pp. 73–95, 1977.

[19] R. Flood, "Classification of sedimentary furrows and a model for furrow initiation and evolution," *Geol. Soc. Am. Bull.*, vol. 95, no. 5, pp. 630–639, 1983.

[20] T. Wiseman, P. Ballin, and M. Lederer, "Multi-Disciplinary Reservoir Description to Characterize Connectivity in a Complex Minibasin Fill: an Integrated Approach at Holstein Field," *Int. Pet. Technol. Conf.*, 2007.

[21] R. T. Beaubouef and V. Abreu, "MTCs of the Brazos-Trinity Slope System ; Thoughts on the Sequence Stratigraphy of MTCs and Their Possible Roles in Shaping Hydrocarbon Traps," *Media*, vol. 28, pp. 475–490, 2010.

[22] L. Moscardelli and L. Wood, "New classification system for mass transport complexes in offshore Trinidad," *Basin Res.*, vol. 20, no. 1, pp. 73–98, Mar. 2008.

[23] R. Wynn and D. A. V. Stow, "Classification and characterisation of deep-water sediment waves," *Mar. Geol.*, vol. 192, 2002.

[24] R. S. Pilcher, B. Kilsdonk, and J. Trude, "Primary basins and their boundaries in the deep-water northern Gulf of Mexico: Origin, trap types, and petroleum system implications," *Am. Assoc. Pet. Geol. Bull.*, vol. 95, no. 2, pp. 219–240, Feb. 2011.

[25] J. Diaz, P. Weimer, R. Bouroullec, and G. Dorn, "3-D Seismic stratigraphic interpretation of quaternary mass-transport deposits in the Mensa and Thunder Horse intraslope basins, Mississippi Canyon, Northern Deep Gulf of Mexico," in in *Mass-Transport Deposits in Deepwater Settings*, 2011, pp. 127–149.

[26] R. Cepeda and P. Weimer, "3D Seismic Stratigraphic Interpretation of the Upper Miocene to Lower Pleistocene Deepwater Sediments of the Thunder Horse – Mensa Area , Southern Mississippi Canyon , Northern Deep Gulf of Mexico," *Gulf Coast Assoc. Geol. Soc. Trans.*, vol. 60, pp. 119–132, 2010.

[27] M. Taylor, "Geohazard assessment 'Thunder Horse' Prospect, Mississippi Canyon Area," 2001.

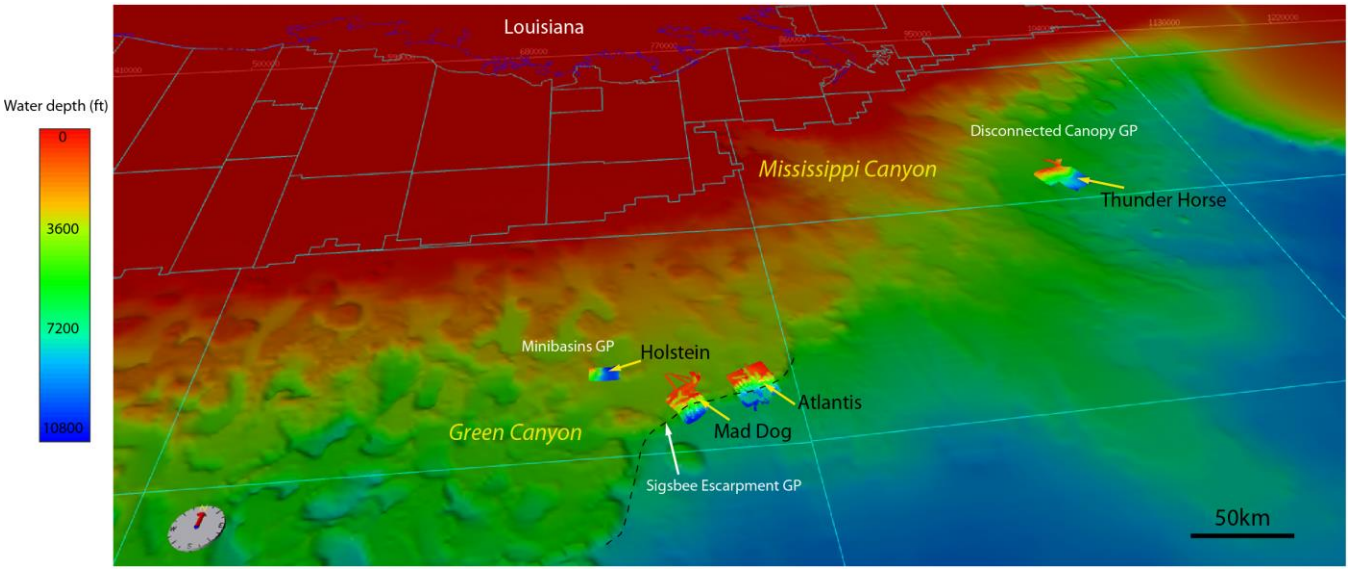

Figure 1. Birds-eye image of the central Gulf of Mexico viewed looking north. Image shows bathymetry overlain with shoreline and block outlines, as well as the outlines of the location of each of the four surveys used in this study and geomorphological provinces (GP). Dashed line marks the Sigsbee Escarpment.

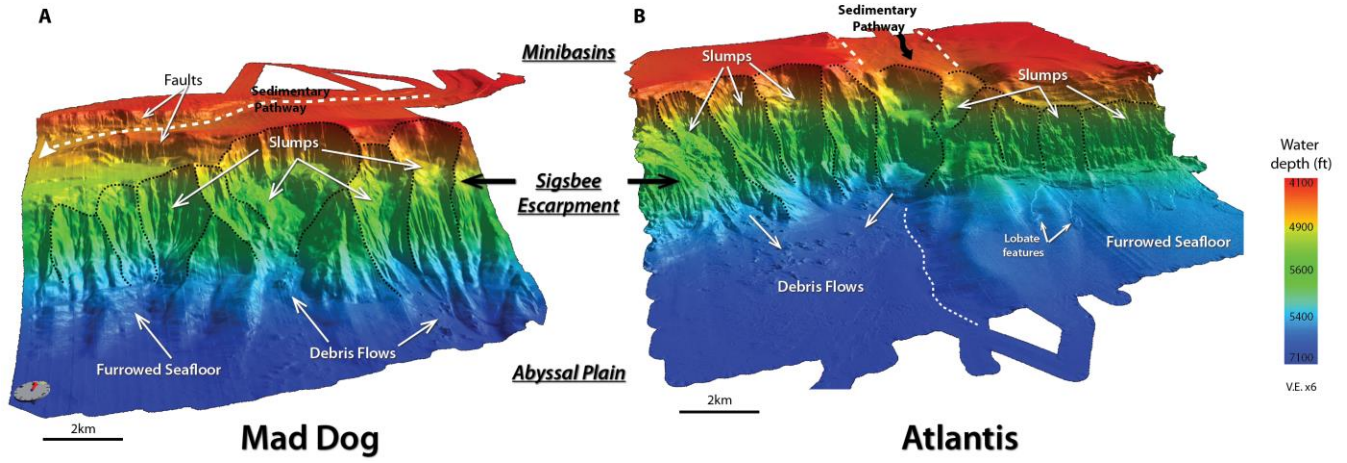

Figure 2. High-resolution, seafloor bathymetry at the Mad Dog and Atlantis survey locations within the Sigsbee Escarpment geomorphological province. The Escarpment is characterized by steep slopes (up to ~40 deg.), a scalloped morphology and abundant slumps and slide scars. In the region landward of the Escarpment; the Minibasin Province, sedimentary pathways are defined by the planform trackways of extensional grabens associated with deflated salt walls and minibasins, and the minibasin lows themselves. Debris flows and erosional furrows characterize the escarpment front and toe of the escarpment. Dashed white lines mark the axis of lows along which sediments are funneled to the escarpment slope and down to the abyssal plain.

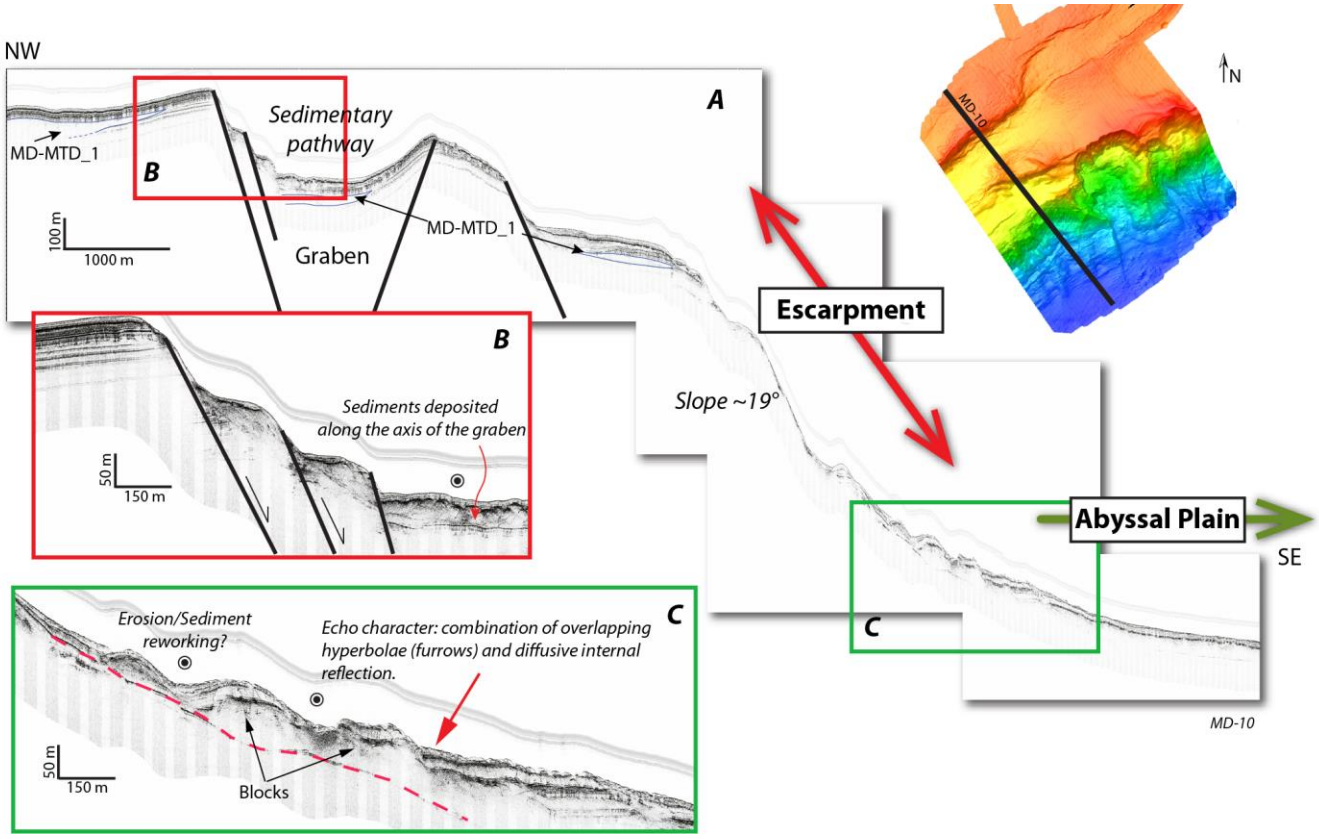

Figure 3. A) Subbottom profile at Mad Dog survey (location shown) showing graben structure above the escarpment, steep slope and slump deposits at the base of the escarpment. B) Close up image along 3A showing the northern sideway faulting along the Mad Dog graben structure. C) Close up image along 3A showing the slumped deposits at the toe so the continental slope and boundary between the slope and the abyssal plain. The red dashed line marks what appears to be a glide track.

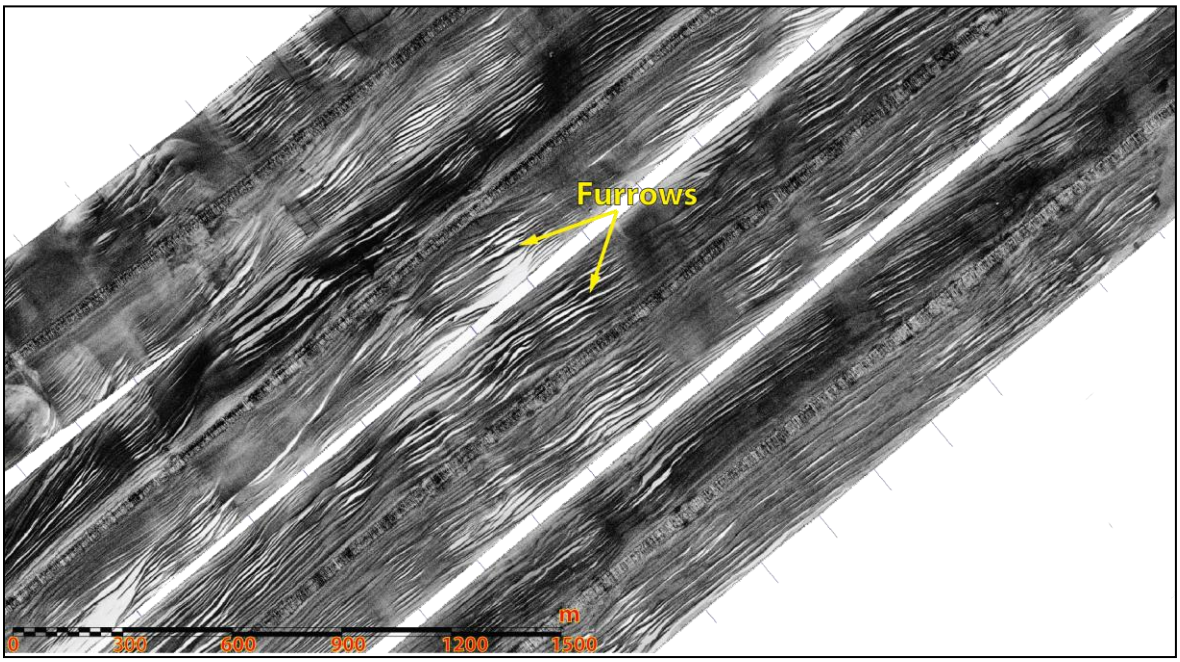

Figure 4. Side scan sonar images at the base of the escarpment in the Mad Dog area showing erosional furrows.

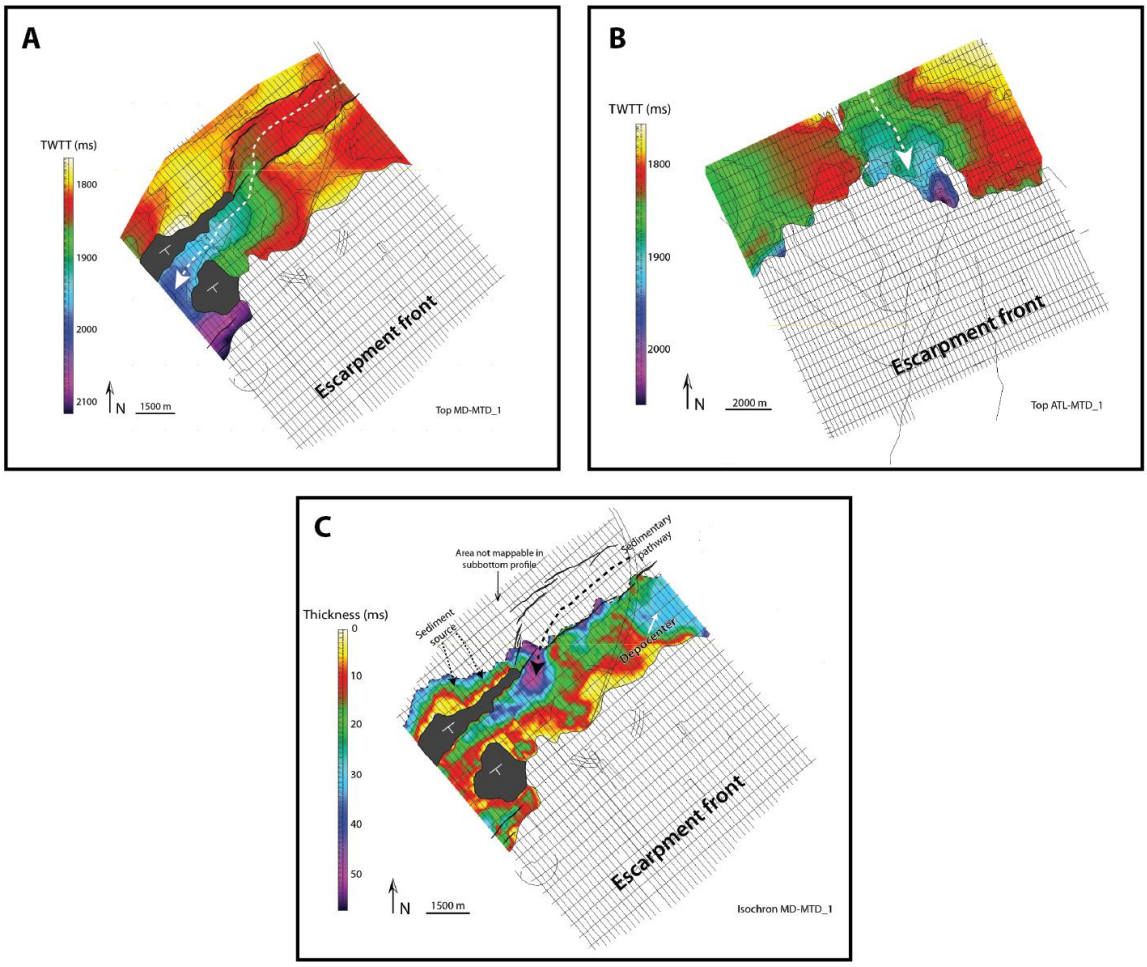

Figure 5. Time structural maps of top surface of MTDs produced from the subbottom profile data in A) Mad Dog and B) Atlantis. This unit is present at the very base of the subbottom profile images that are collected over these areas (see Fig. 3A). The isochron map at Mad Dog (C) shows a NE-SW oriented sedimentary pathway that is controlled by the underlying graben structure. The NE-SW trending elongated depocenter is confined within the graben structure above the escarpment.

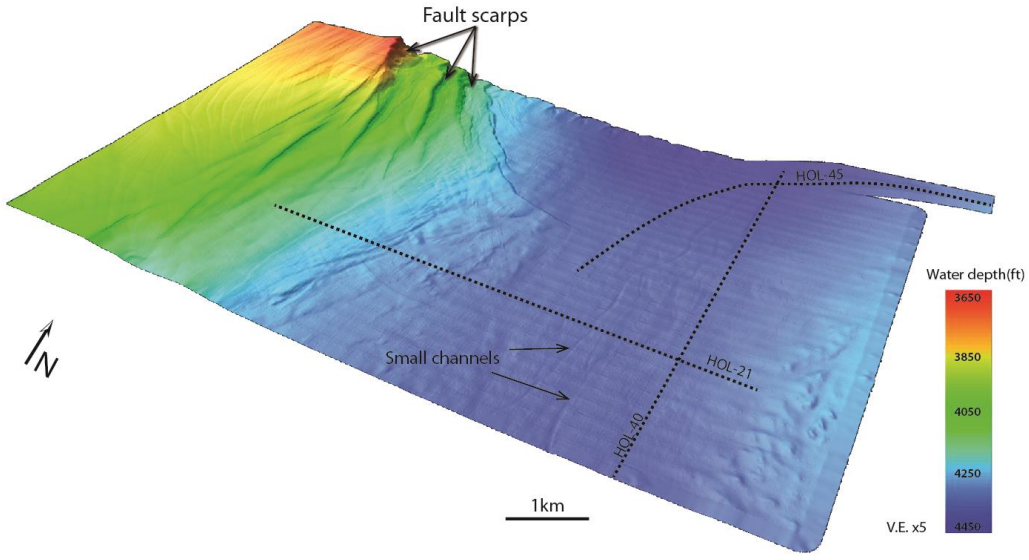

Figure 6. Bathymetry over the Holstein survey. Location shown on figure 1. Faults are visibly displacing the seafloor and track paralleling the western margin of a bathymetric low where channels are visible in bathymetry image.

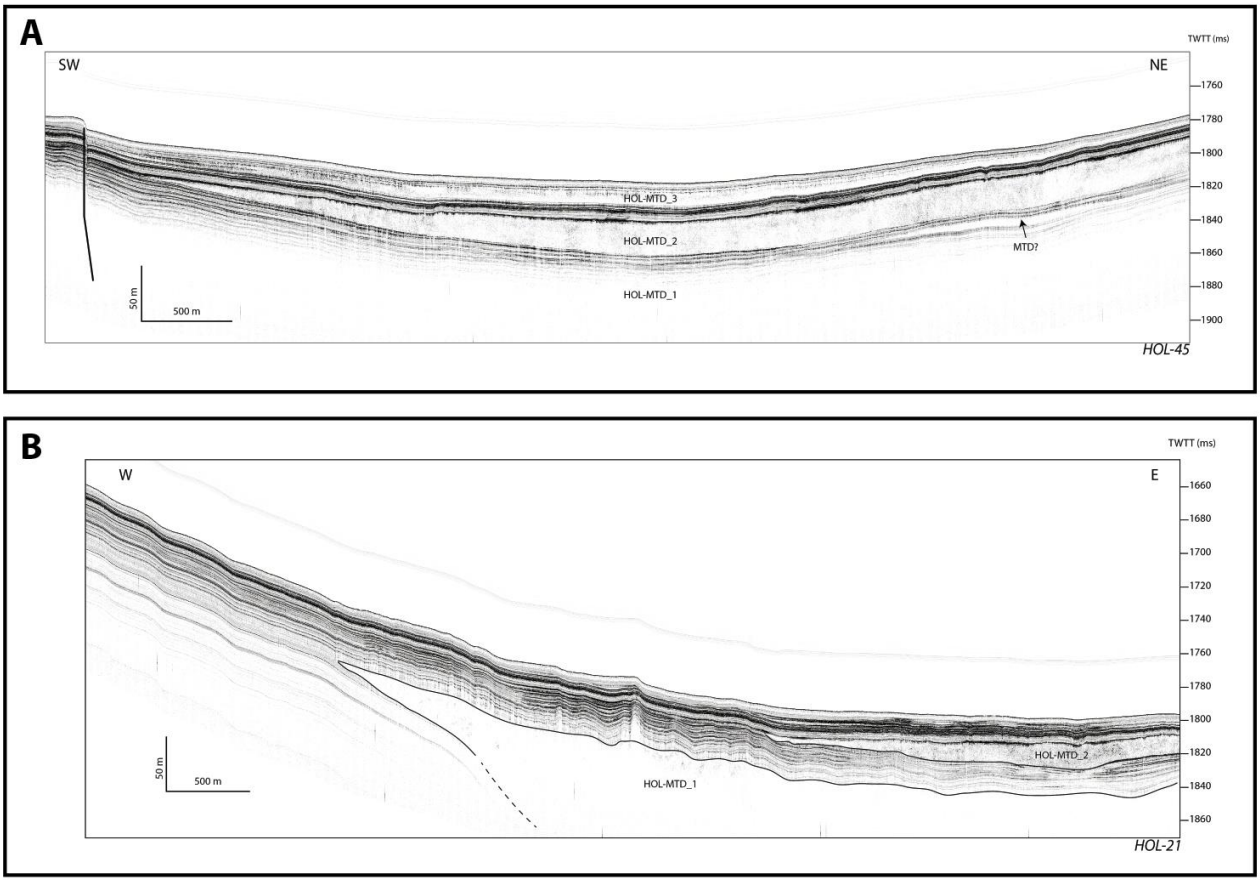

Figure 7. Two subbottom profiler lines extracted from the Holstein data survey. Locations are shown in figure 6. A) The profile shows a ponded configuration with the intercalation of packages of parallel continuous reflectors, and packages of chaotic semi-transparent reflectors, here interpreted to represent mass transport deposits (MTDs). B) MTDs can be seen truncating the well defined high amplitude parallel continuous reflector package beneath it.

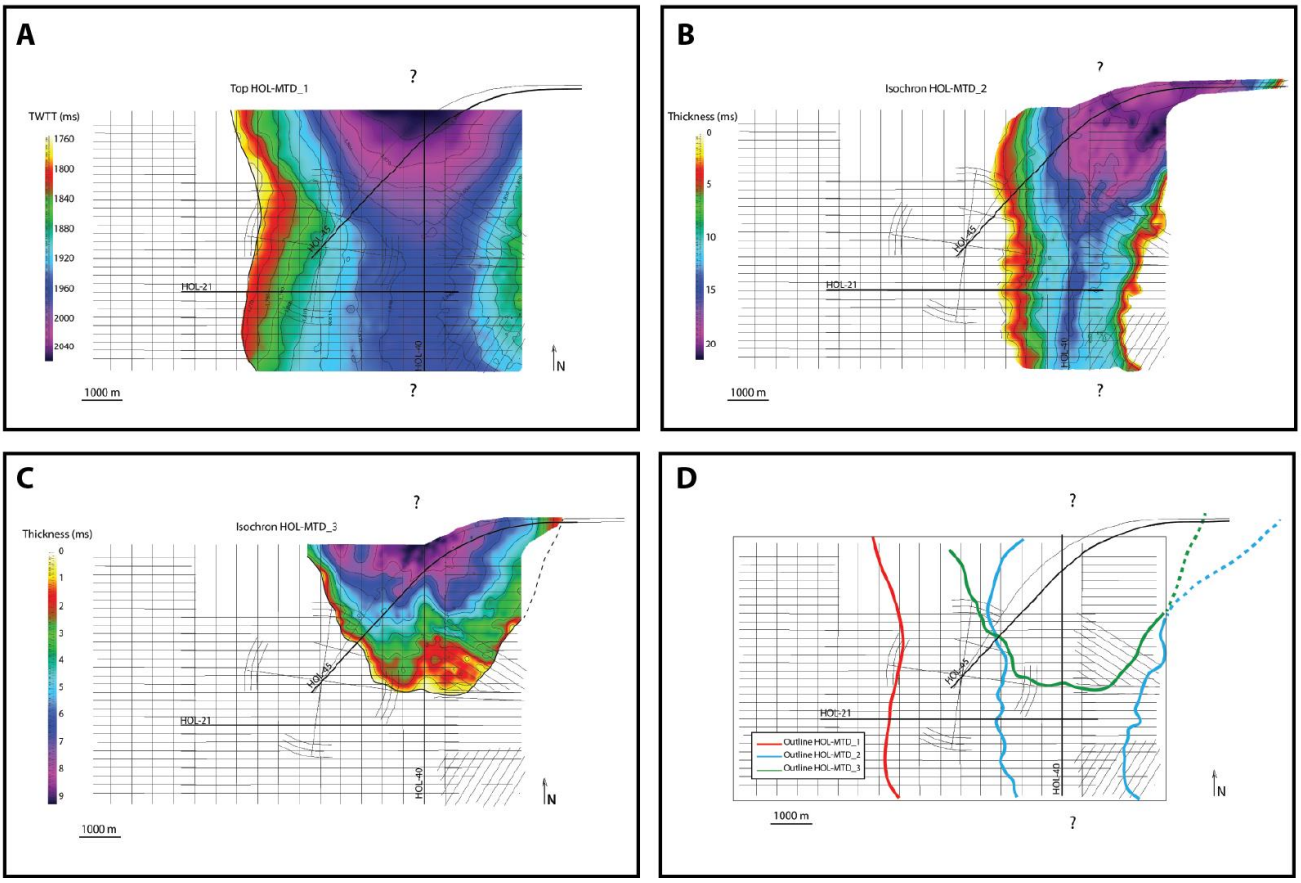

Figure 8. A) Time structural map of top of HOL-MTD_1. The unit wedges to the west. The extent of the unit reaches outside the minibasin to the south. B) Isochron map of HOL-MTD_2. The unit shows a depocenter to the north and a narrow conduit to the south. It wedges to both west and east edges of the minibasin. C) Isochron map of HOL-MTD_3. The unit shows a depocenter to the north and its extent is confined within the minibasin. D) Outline of the three MTDs mapped. The figure shows how the MTDs become narrower and smaller in size from older to younger.

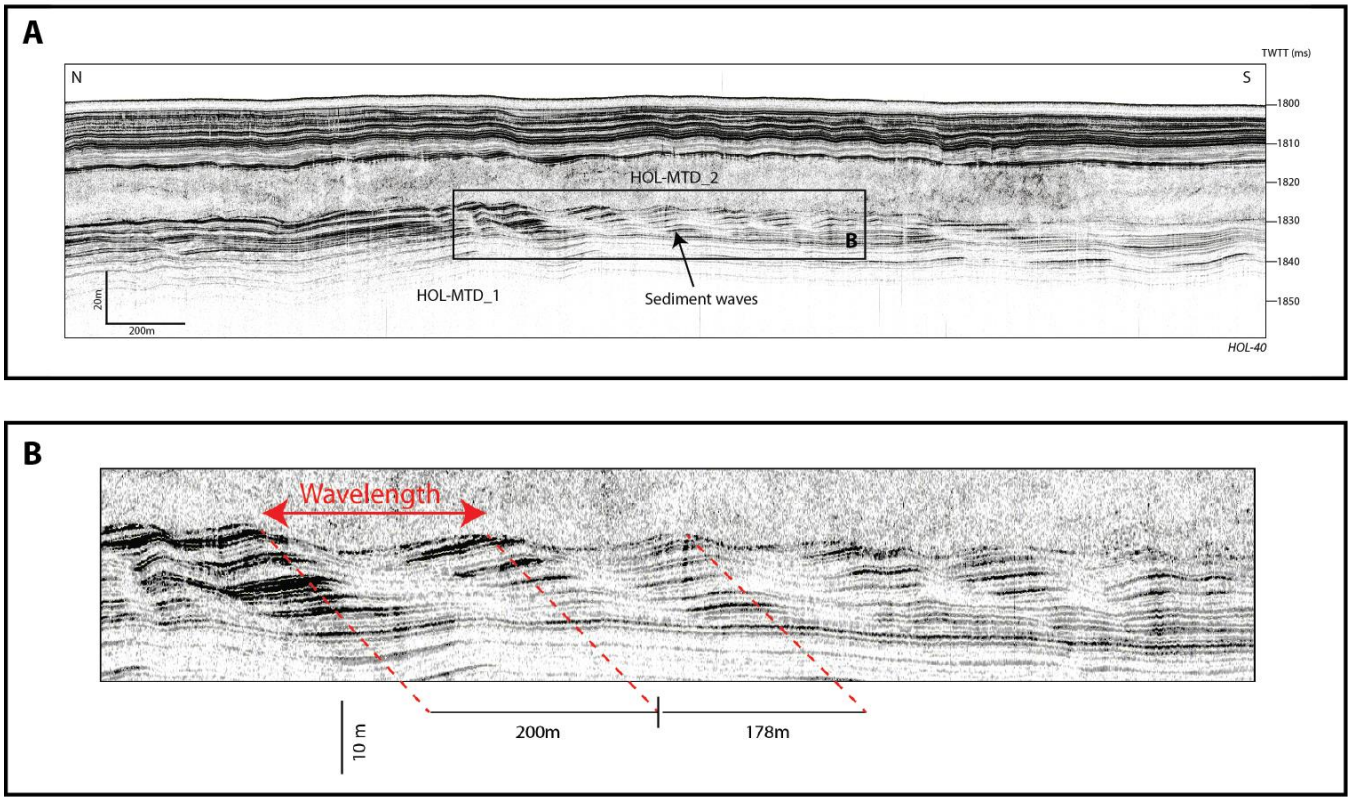

Figure 9. A) Subbottom profiles showing sediment waves below HOL-MTD_2. Location is shown in figure 6. There appears to be truncation of the uppermost wave set. However the MTD does not appear to have done this erosion since the overall topography of the wave set surface is retained. The light and dark alternations suggest the deposits are alternating temporally between high and low reflectivity material, possibly coarser, high reflectivity sands and finer, low reflectivity muds. B) Image showing the crest to crest measurement methodology of sediment wave train morphometrics.

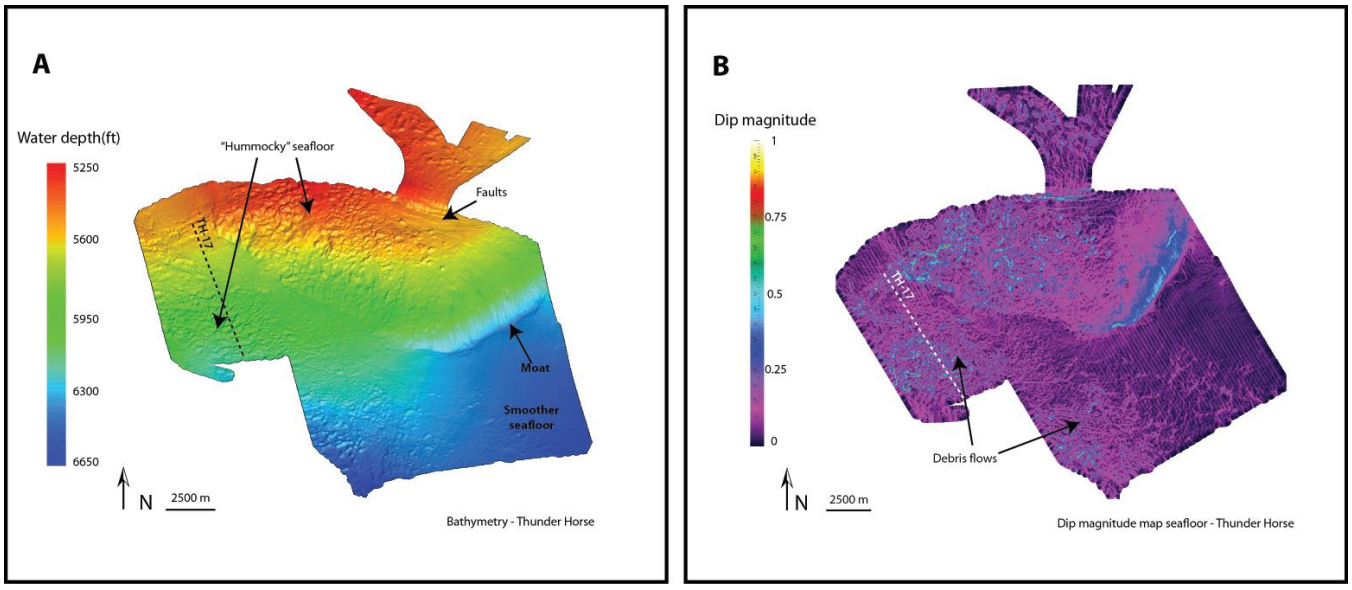

Figure 10. A) Bathymetry at Thunder horse survey. The texture of the seafloor is "hummocky" in some areas and there is a transitional area that defines the boundary between the domal structure to the east and the lower elevations where the seafloor is smoother. B) Dip magnitude map of the seafloor. The presence of debris flows moving downslope is highlighted.

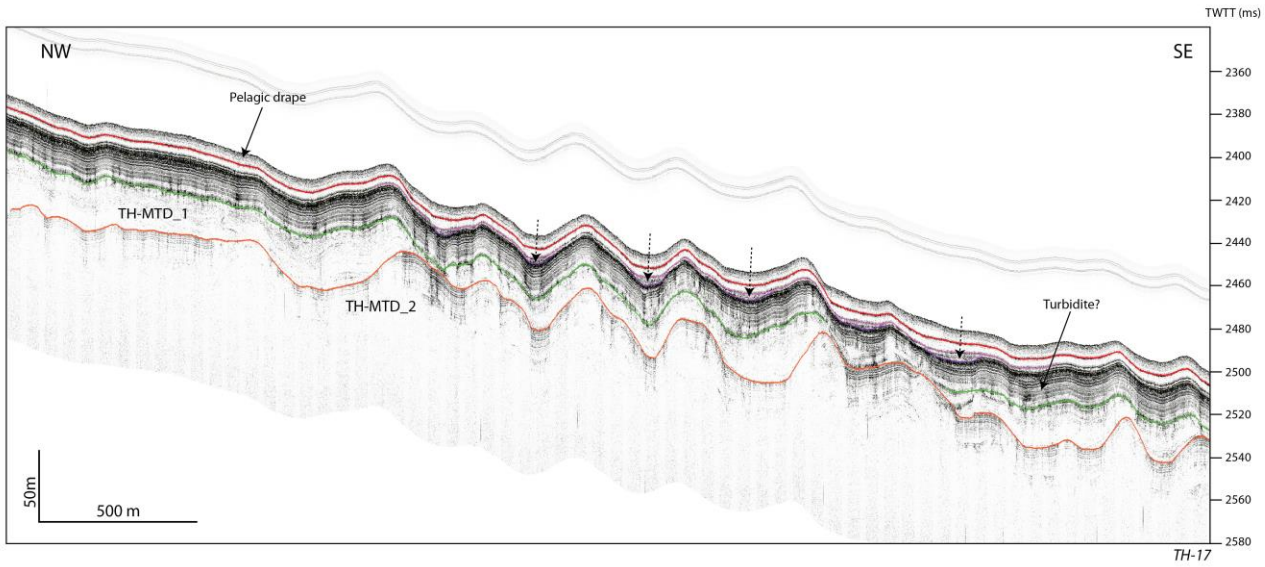

Figure 11. Subbottom profile TH-17 at Thunder Horse. Location is shown in figure 10. The profile shows the presence of two MTDs (TH-MTD_ 1 and TH-MTD_2) and possible turbidite deposits. Uneven thickness in some units is seen as a result of previous inherited "hummocky" topography (see dashed arrows).